LATIN AMERICAN CUBESAT WORKSHOP
SALVADOR, BR
OCTOBER 2024

The influence of different scenarios on the temperature response of CubeSat's battery

Felipe Teodormo Mendes[1], Maria Eduarda Emiliano Rezende[2], Caique Sales Miranda Gomes[2], Laio Oriel Seman[3], Elaine Maria Cardoso[1], and Edemar Morsch Filho*[1]

[1]Department of Aeronautical Engineering, São Paulo State University - UNESP
[2]Department of Mechanical Engineering, Federal University of Santa Catarina - UFSC
[3]Department of Automation and Systems Engineering, Federal University of Santa Catarina - UFSC

Abstract

Before a CubeSat starts to operate in orbit, several tests are performed to ensure its subsystems work according to design specifications. In this sense, numerical simulations are a fundamental tool for testing representative operating scenarios, which are often difficult to reproduce in the laboratory, especially because of the microgravity environment, vacuum, temperature, and radiation levels found in space. In a satellite project, including CubeSats, some questions to be answered before the satellite is even manufactured include its temperature in orbit, especially the battery, which is one of the most temperature-sensitive components and usually requires thermal control to prevent failures. Operating the battery in temperature ranges outside those recommended by the manufacturer can increase its degradation or even cause permanent failure, which puts the entire mission at risk. The temperature scenario in which a CubeSat is exposed depends directly on its orbit and attitude, which also impacts the temperature field of the battery. However, internal heat generation occurs naturally during battery operation and must be considered in thermal modeling. This phenomenon depends, among other factors, on the current drawn and the time it is being used. This work seeks to thermally model in CFD (Computational Fluid Dynamics) the thermal behavior

*Corresponding author: edemar.filho@unesp.br

of a battery integrated into a CubeSat to obtain the battery's temperature scenarios. To achieve this, the thermo-electrical modeling of the battery and the thermal modeling of the CubeSat are created and solved in the Ansys CFX software. Different orbits and currents are considered in the analyses to present possible temperature scenarios for the battery, which can assist in the planning and development of the Electrical Power System (EPS) and Thermal Control subsystem of a CubeSat mission. The results indicate scenarios in which attention should be paid to the thermal management of the battery to avoid temperatures that are too low, and this could be used to design the thermal control subsystem.

1 Introduction

The first CubeSat launch, which is a category seen within nanosatellites, took place on June 30, 2003, placing Danish, Japanese, Canadian, and North American nanosatellites into orbit. The first use of a CubeSat for a scientific mission came through NASA's Ames Research Center. In 2006, the *Biological CubeSat* group launched GeneSat-1 to conduct biological experiments in space and the success of the mission resulted in great acceptance of the idea of nanosatellites and CubeSats by the scientific community [1].

According to [2], in its study on the failure rate in small satellites, by the year 2016, 41.3% of all satellites in this category faced total or partial failures, with 6.1 % of these failures caused by failures in the launch vehicle, 11% correspond to partial failures of the nanosatellite and the remaining 24.2% represent total failures of the space mission.

In this sense, it is worth noting that the increased complexity in the requirements of modern space missions has also resulted in new challenges for the operation, maintenance, and longevity of missions using satellites. Thus, the use of nanosatellites makes the problem even more challenging, for example, due to their limited mass, volume, and external area available for the allocation of photovoltaic panels for energy generation, dissipation of heat, and for integration of different subsystems that would be usual for large satellites [3, 4].

Therefore, to carry out tests and analyzes before launch are extremely important to reduce any risks that could make the space mission unfeasible. In other words, it is essential for the success of missions to carry out several CFD (Computational Fluid Dynamics) simulations aimed at sizing subsystems and verifying their operation, as well as helping to obtain adequate behavior while in orbit.

Given the above, the main objective of this work is to numerically simulate the heat transfer in a CubeSat, focusing on the temperature achieved at solar panels and batteries for different orbit scenarios.

2 Bibliography review

Regardless of the size of the satellite, in general, they are all made up of a set of subsystems, as indicated in Fig. 1. Each of these subsystems has a function within the mission, but only the Electrical Power System (EPS) and Thermal Control will be highlighted here.

The objective of the EPS is to generate, store, regulate and distribute the electrical energy that the satellite needs to complete the mission requirements. It is divided into primary and secondary energy sources, represented by solar panels and batteries, respectively. So-

Figure 1: CubeSat's subsystems

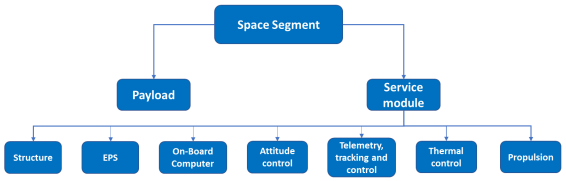

lar panels correspond to the arrangement of dozens of individual solar cells, capable of generating from a few watts to tens of kilowatts. Batteries are used for the secondary energy generation system, providing it in periods when the primary system is not available, such as during eclipse phases. In this way, the batteries provide energy during the absence of solar incidence on the satellite and are recharged during the period in which there is incidence [5].

The objective of thermal control is to guarantee the operation of electronic and mechanical equipment within the operating temperature limits, efficiently and reliably. In general, electronic equipment in space needs to be kept in a temperature range between -15°C and +50°C, while batteries must be kept between 0°C and +20°C [6].

To develop the thermal control of a satellite, a fundamental step is to estimate the heat transfer it will have in orbit. To this end, in the initial development stage of CubeSats projects, the analytical formulation approach provides general results, with great agility and low cost. However, as the project moves into more advanced phases, approaches with more precise formulation become necessary. For this reason, numerical simulations are widely used to understand the behavior of nanosatellites, being capable of generating results with high accuracy and levels of detail [7]. Among the numerical methods available and most used for these problems, there is the Finite Difference Method (FDM), the Finite Element Method (FEM), and the Finite Volume Method (FVM).

The work of [8] shows that passive thermal control is more than sufficient to keep electronic components for aerospace use within their recommended operating values, as seen in Tab. 1. To reach this conclusion, the authors implemented thermal simulations in MATLAB using FEM, where the temperature conditions for multiple orbits and their extremes were evaluated.

Table 1: Operational temperature of subsystems [9].

Components	T_{min} [ºC]	T_{max} [ºC]
Electronics (PCB)	-40	+85
Battery (charge)	0	+45
Battery (discharge)	-40	+60
Structure	-40	+85
Solar panels	-100	+100

In the work of [9], the authors computationally analyzed nanosatellites operating at altitudes between 500 km and 2000 km, considering a passive thermal control system, also obtaining satisfactory results for all electronic components, with the exception of the battery. The authors employed a nodal model based on energy conservation. The work also showed that the temperatures of photovoltaic panels are extremely sensitive to the type of material used in the surface coating of the panels. However, as also observed in [8], the authors emphasize that for extreme negative temperature conditions, the use of heaters for the batteries is recommended to guarantee operability in all conditions during orbit, especially during the eclipse phase.

The studies carried out by [10] and [11] also simulate CubeSats in orbit, and these authors employ equivalent resistances to model thermal behavior. For the first work, the author compared the results obtained by using equivalent resistances with an analysis carried out in the *ESATAN-TMS* software, obtaining the same temperature distribution for both analyses. For the second study, a software tool was developed based on the equivalent resistance technique, focusing on modeling the thermal behavior of small satellites, being used to evaluate the performance of the Canadian Space Agency's CASTOR satellite, obtaining a difference less than 5% in the satellite's surface temperatures.

Thermal analyses were also performed to estimate the performance of the nanosatellite, developed by students at the University of Texas. In this project, participants carried out experimental thermal cycle tests and thermal analyses, with the thermal cycle being carried out in Chamber-N at the Johnson Space Center, for extreme cold and heat scenarios, while thermal analyses were carried out using the Method of Finite Elements [12]. Among the results, there were temperature peaks that were similar between the model and the data from the experimental tests, with the use of a thermal blanket being used to help maintain the satellite's thermal balance in extreme cold conditions, but which was not able to avoid battery overheating in extreme heat condition.

Through a thermal model developed in Matlab, [13] aimed to evaluate and verify compliance with the requirements established for the mission of the Falconsat-2 program in 2001. Through the tool developed in Simulink, it was possible to choose an approach for thermal control, based on compiling a history of external flow inputs to the satellite in an orbit, later using them to analyze the thermal behavior of the satellite in orbit, using the FDM. At the end of the work, a passive thermal control edge was chosen using aluminum and Kapton tape on the faces of the external structures, as this proved to be capable of keeping the components operating within the temperature specifications desired for the project.

The work of [7] focused on the transient thermal simulation of a 1U CubeSat, where the heat transfer by conduction and radiation (external and internal) were solved using the FVM. To solve the internal radiation in the CubeSat, the Gebhart method and an obstruction model were implemented, and three conditions for the internal emissivity were tested. The results showed a significant impact of the internal heat transfer by radiation on the temperature field of the entire satellite, and comparisons with a simpler nodal model showed good agreement, although the latter did not consider three-dimensional effects.

3 Methodology

The problem to be solved is based on the geometry of the CubeSat 2U called GOLDS-UFSC, which is presented in Fig. 2. This CubeSat is under development at SpaceLab (`https://spacelab.ufsc.br/en/home/`) and is scheduled to be launched in 2025.

From this model, the geometry to be used in the simulations of this work was created, as seen in Fig. 3, which is composed of 2 main aluminum structures (gray), each measuring 100 mm $\times$ 100 mm $\times$ 100 mm. Internally, it has four corners for fixing Printed Circuit Boards (PCBs) to the structure using screws, these being representative of the dif-

Figure 2: CubeSat GOLDS-UFSC [14].

(a) External (b) Internal

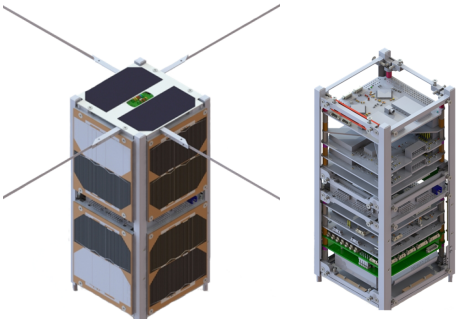

ferent electrical and electronic subsystems of the nanosatellite. The nanosatellite has four PCBs (green) for each floor U, with 80 mm $\times$ 80mm $\times$ 2 mm each. In the center of a PCB of each CubeSat unit there is a battery, represented by the dark blue component. Furthermore, in order to minimize problems arising from radiation encountered in orbit on the electronic components, there are shields made of aluminum (yellow) for each of the satellite's faces, each measuring 100 mm $\times$ 100 mm $\times$ 3 mm. Finally, the photovoltaic panels (light blue) are attached to the outer face of each of the shields, and aim to transform the incident solar radiation into electrical energy to power the nanosatellites various subsystems.

3.1 Mesh and simulation parameters

A mesh independence test was performed to verify the convergence of the simulation. Three meshes were created, with a total of 72,366, 214,153, and 522,089 cells. To verify the influence of the mesh on the results, the temperature on the +X and +Y panels were monitored in a prescribed flow condition over the faces. The results obtained through this

Figure 3: Main CubeSat's parts

(a) Internal view (b) Structure

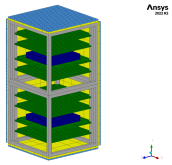

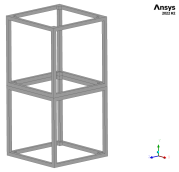

(c) Internal parts (d) Solar panels

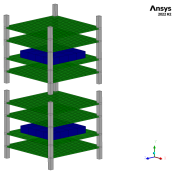

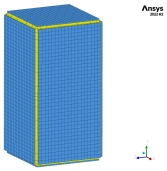

analysis are in Tab. 2. As a result of the mesh independence test, it was decided to carry out the case studies of this research with Mesh 2, as it presents the best relationship between computational cost and accuracy among the evaluated meshes.

Table 2: Mesh independence test

Mesh	N° of cells	T_{+X} [°C]	T_{+Y} [°C]
1	72.366	7.23	6.53
2	214.153	8.12	6.72
3	522.089	8.20	6.77

As a time step, 10 s was used, and around 15 complete orbits were simulated until a response with a cyclic pattern was reached. To present the results, only the last orbit is considered. As a convergence criterion, a residual (RMS) of $10\times^{-7}$ was used for the energy equation.

3.2 Heat transfer

In order to simulate heat transfer in the CubeSat in orbit, an energy balance will be used, considering the assumptions of transient

regime, constant material properties, and perfect vacuum, according to Eq. 1:

$$\rho c_p \frac{\partial T}{\partial t} = k\nabla^2 T + \dot{q} \quad (1)$$

where ρ is the density [kg/m^3], c_p is the specific heat at constant pressure [J/kg.K], T is the temperature [K], t is the time [s], k is the thermal conductivity [W/m.K] and $\dot{q}$ is the source term.

In this work, the heat transfer that occurs in the CubeSat involves only conduction and radiation transfer modes. However, the internal heat exchange by radiation will be ignored as this phenomenon requires calculations of obstructions and reflections, which requires a more sophisticated formulation. In order to simplify the analyses, this work assumes that all external surfaces of the CubeSat are opaque, gray (radiation independent of wavelength), and diffuse (radiation independent of direction).

3.3 Boundary conditions

The boundary conditions involved in the CubeSat's heat exchange are based on four forms: absorption of solar flux, albedo, and infrared, in addition to its own emission. Each of these terms is modeled according to the work of [15].

The material properties used in the thermal simulation are listed in Tab. 3.

The values used for the absorptivity and emissivity of the surfaces will be discussed later, together with the definition of the case studies.

Table 3: Material properties [15].

Component	k	c_P	ρ
Structure	140	948	2810
PCB	1.03	1103	2325
Battery	21	933	2122
Shielding	140	948	2810
Solar panel	1.03	1103	2325

3.4 Heat generation at the battery

Aiming to understand the thermo-electric behavior of batteries typically used in CubeSat projects, the proposed model by [16] was implemented. It is worth noting that in the analyses, the electrical behavior of the battery does not interfere with the electrical model of the photovoltaic panel, nor vice versa.

The battery's heat generation rate, $\dot{q}_b$ [W/m^3], is given by:

$$\dot{q}_b = \frac{I}{V_b}\left[IR + T\frac{\partial U_O}{\partial T}\right] \quad (2)$$

where V_b is the battery volume [m^3], I is the charge and discharge current [A], R is its resistance [Ω], T is the battery temperature and $\partial U_O/\partial T$ is the thermal entropy coefficient.

According to [17], the thermal entropy coefficient, in the unit of millivolts, can be obtained by:

$$\frac{\partial U_O}{\partial T} = -0.355 + 2.154 \times SoC - 2.869 \times SoC^2 + 1.028 \times SoC^3 \quad (3)$$

where SoC (State of Charge) indicates how much charge capacity remains in the battery, with the maximum value being 1 (full battery) and the minimum being 0 (empty battery).

The general equation for the SoC is:

$$SoC = SoC_{in} - \frac{It}{Q_c} \quad (4)$$

where SoC_{in} is the initial charge value [-], Q_c is the nominal battery capacity [Ah] and t is the time [s]. To complete the model, according to [18], the electrical resistance of a battery is not constant, varying according to its temperature and state of charge (SoC), and can be calculated in mΩ. In this work it is assumed that the battery capacity (Q_c) is 2 Ah and the initial state of charge (SoC_{in}) is 1, that is, the battery is always initially fully charged. Although the other electronic components of a satellite also end up generating heat during its operation, these will be disregarded in this work.

3.5 Study cases

In terms of orbit, two configurations will be evaluated: with and without eclipse. In order to evaluate representative CubeSat scenarios, the orbit is 506 km high, circular, and has an inclination of 90°.

For each orbit, two attitude conditions will be evaluated, that is, CubeSat pointing and rotation, which here will be called Nadir (N) and Maximum Projection (MP). For the Nadir scenario, the CubeSat constantly points one of its faces towards the center of the Earth, while the Maximum Projection case consists of a configuration where the CubeSat constantly maintains three of its faces towards the Sun.

4 Results

Figure 4 shows the temperature at the center of each panel and the CubeSat battery throughout a complete orbit, for varying attitude and orbit conditions.

Figure 4: Solar panel and battery temperature for $\alpha = 0, 3$, $\epsilon = 0, 3$ and $I = 0$ A

(a) Orbit with eclipse - Nadir attitude

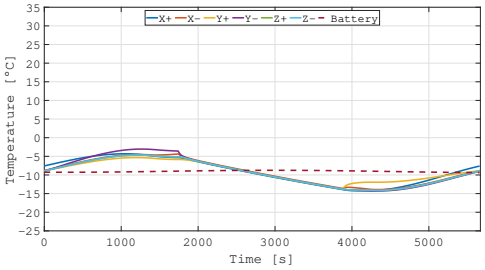

(b) Orbit without eclipse - Nadir attitude

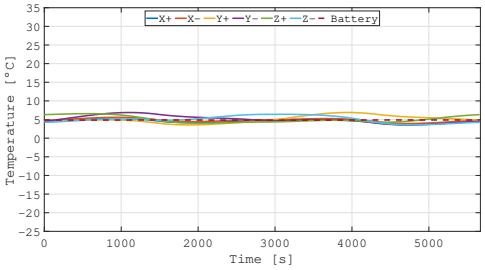

(c) Orbit with eclipse - MP attitude

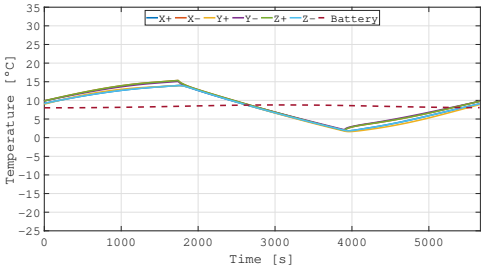

(d) Orbit without eclipse - MP attitude

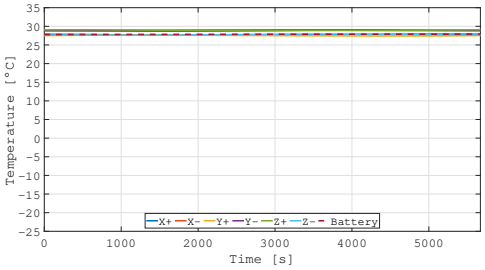

Although the CubeSat is 2U, with ten photovoltaic panels and two batteries, the results indicated that the temperatures on the same side are very close and, therefore, it was decided to show only one panel on each side. For batteries, the temperatures are also very close and therefore only one will be shown. In all cases of Fig. 4 there is an absorptivity (α) and emissivity (ϵ) of 0.3 for both, in addition to a null current (I) passing through the battery.

Analyzing the behavior of the Fig. 4 curves, it is noted that the lowest operating temperatures occur for the Nadir scenario with eclipse, while the highest operating temperatures are for the Maximum Projection attitude without eclipse. This behavior results from the magnitudes for the total thermal radiation fluxes over the CubeSat. Although the thermal radiation peak is greater for the Nadir attitude, the Maximum Projection case has more surfaces facing the sun simultaneously. For all observed cases, the battery temperature is practically constant throughout the orbit, being approximately an intermediate value between the absolute temperature extremes of the photovoltaic panels. This behavior can be explained by the thermal inertia of the batteries combined with the fact that the thermal loads on them are less intense, precisely because they are located inside the CubeSat. It is worth noting that the thermal radiation fluxes only affect the external faces of the CubeSat, that is, only on the photovoltaic panels, while internally the modeling of the problem assumes a zero exchange for radiation. In this way, the temperatures of the batteries result only from the exchange of heat through conduction, which reaches them through the internal structure of the CubeSat, and from its internal generation of heat when a current passes.

Cases without an eclipse present higher temperature levels when compared to cases with an eclipse, this being an expected result because, throughout the time that the CubeSat is under the earth's shadow, it stops receiving thermal radiation of the solar-type and albedo, which are the most significant, respectively. In fact, the lowest temperatures are associated with the last moment in which the satellite is under the Earth's shadow. Furthermore, it is observed that the cases evaluated in Fig. 4 indicate that the greatest temperature variations throughout an orbit occur for the Nadir attitude, this result being explained due to the greatest variations in the total radiation flux for this case.

Table 4 highlights the maximum and minimum temperatures of solar panels obtained for each of the attitude and orbit conditions analyzed so far, where it is possible to verify that the highest temperatures are obtained for the Maximum Projection scenario without the occurrence of an eclipse. The maximum temperature is approximately 29°C, while the minimum is -15°C for the case with eclipse at Nadir attitude.

Table 4: Extreme temperatures

Case	T_{max} [°C]	T_{min} [°C]
N with eclipse	-3,05	-14,30
N without eclipse	6,88	3,56
MP with eclipse	15,30	1,62
MP without eclipse	28,85	27,90

In order to compare the impact of the absorptivity and emissivity of photovoltaic panels on their temperature, simulations were also carried out for two different conditions of these parameters. The scenario chosen to be analyzed was the Nadir with eclipse because the satellite presents a more dynamic behavior for

incident radiation flows. The results of this analysis consider that there is no current passing through the battery (I=0 A) and they are in Fig. 5.

Figure 5: Solar panel and battery temperature, orbit with eclipse and Nadir attitude

(a) α = 0,3 and ϵ = 0,7

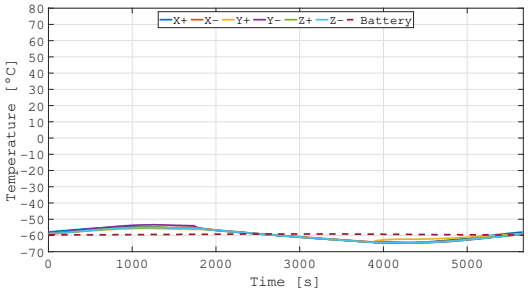

(b) α = 0,7 and ϵ = 0,3

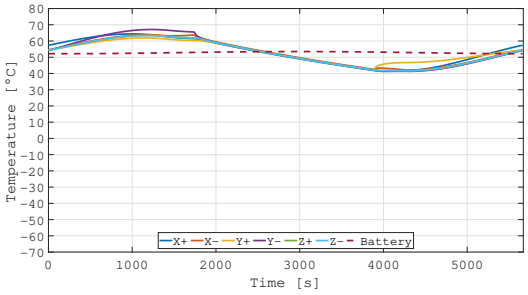

It is possible to note, as expected, that absorptivity and emissivity have a direct relationship with the temperature reached by the satellite's photovoltaic panels. The most extreme cases are found in conditions where the values between constants differ. The results indicate that a low ratio for α/ϵ, that is, the lower the absorptivity and the higher the emissivity, result in a lower temperature reached by the panels, as observed in Fig. 5a. On the other hand, the higher the absorptivity of the panel and the lower the emissivity, that is, a high ratio of α/ϵ, the hotter the panel will be, as shown in Fig. 5b.

According to Tab. 5, the hottest solar panel temperatures are obtained for the condition of highest absorptivity and lowest emissivity, that is, when the satellite has a high capacity to absorb heat, but is unable to emit it. On the other hand, for the scenario where emissivity is higher than absorptivity, the satellite ends up being more likely to lose heat with the environment, thus justifying the low temperatures observed.

Table 5: Extreme temperatures for different absorptivities and emissivities

Case	T_{max} [°C]	T_{min} [°C]
$\alpha/\epsilon = 0,3/0,7$	-53,40	-64,60
$\alpha/\epsilon = 0,7/0,3$	67,09	41,27

To discuss the thermal results relating to the use of the battery, it is first necessary to illustrate its operation. In this work it was considered that the battery would only be used when the CubeSat was under the Earth's eclipse, therefore scenarios without an eclipse are not addressed here, and no assessment related to its charging was carried out. To illustrate the analysis, only the Nadir attitude scenario with eclipse will be discussed for different currents passing through the battery. The occurrence of these currents in CubeSats was not evaluated and was only used to demonstrate the scope of the simulations in this work.

Figure 6 shows the battery's operating relationship and the behavior of the SoC (Eq. 4). Until the eclipse starts, the SoC for the 3 currents remains at its maximum value of 100% and the battery remains disconnected. After the start of the eclipse at time 1740 s, the battery is turned on, and this behavior is represented by the ascending step function of the red line. The SoC is represented by

blue for 0 A, green for 1.25 A, and purple for 2.50 A. It is possible to visualize a descending straight line of the SoC during the eclipse phases, demonstrating the reduction in the charge stored in the battery, reaching minimum values of 63% and 28% for I = 1.25 A and I = 2.50 A, respectively. After the end of the eclipse at 3900 s, the battery is turned off, illustrated by the red line returning to value 0, while the SoC gradually returns to the 100% state by accumulating the excess energy generated by the photovoltaic panels, although this situation was not addressed in this work.

Figure 6: Battery operation and SoC through the orbit

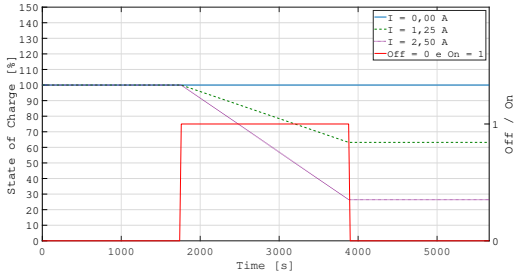

Analyzing Fig. 7, an expected behavior can be confirmed, which consists of higher temperature values when using higher currents. This behavior can be seen in both absorptivity and emissivity parameter scenarios, with the temperature for the highest current in Fig. 7a being on average 40% higher than the case without any current, resulting in an increase in approximately 30°C. For Fig. 7b, which corresponds to the hottest scenario, the battery temperature for a constant current of 2.50 A is 27% higher than that of 1.25 A and 35% for the case without no current.

These results indicate that the thermal analysis of a CubeSat battery must take into account the current passing through it, and it is

Figure 7: Battery temperature for different currents

(a) $\alpha = 0{,}3$ and $\epsilon = 0{,}7$

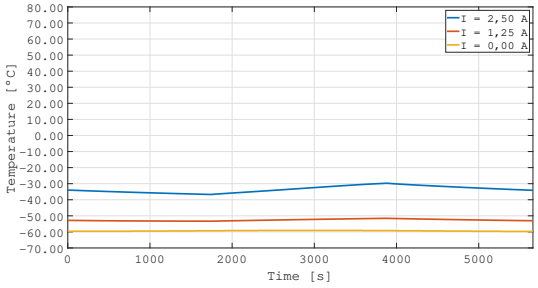

(b) $\alpha = 0{,}7$ and $\epsilon = 0{,}3$

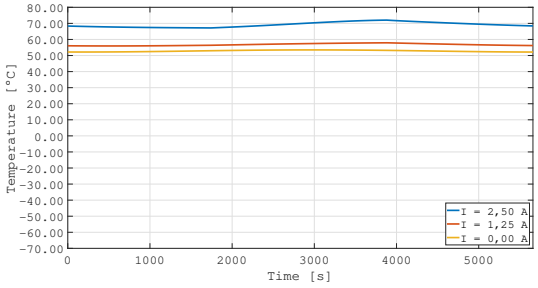

necessary to know the magnitude over time.

5 Conclusion

Based on all the results obtained through computer simulations for the various attitudes and orbits, it was possible to see that these are responsible for generating a significant impact on the satellite's thermal scenarios. Therefore, the correct dimensioning of the components is extremely important for the satellite to be able to fulfill its mission. In addition, it was possible to verify that the battery represents the greatest potential risk of the electronic components since when exposed to extreme cold and heat conditions, it exceeds the thermal specifications determined by the manufacturers. The results indicated that surface parameters such

as absorptivity and emissivity directly impact the CubeSat's temperature, and promote very different levels, depending on their combination.

Finally, simulations involving the battery also reinforce the need for the thermal and electrical areas to be integrated and resolved in a single model to estimate their behavior.

Acknowledgements

The authors are grateful for the financial support from Conselho Nacional de Desenvolvimento Científico e Tecnológico (grants number 117582/2024-7).

References

[1] Space Foundation, "Cubesats," 2022, https://www.spacefoundation.org/space_technology_hal/cubesats/.

[2] S. A. Jacklin, "Small-satellite mission failure rates," *NASA Ames Research Center*, p. 46, 2019.

[3] F. D. P. M. JUNIOR, "Avaliação do uso de tubos de calor para o controle térmico em nanossatélites," Joinville, Santa Catarina - Brasil, 2017, dissertação de mestrado.

[4] J. T. Sebastian and V. Y. Baby, "Numerical investigation of thermal energy storage panel using nanoparticle enhanced phase-change material for micro satellites," *International Research Journal of Engineering and Technology (IRJET)*, vol. 5, no. 4, pp. 2330–2335, 2018.

[5] C. Cappelletti, S. Battistini, and B. Malphrus, *CubeSat Handbook: From Mission Design to Operations*. London Wall, London - United Kingdom: Academic Press, 2020.

[6] P. Fortescue, G. Swinerd, and J. Stark, *Spacecraft Systems Engineering, 4h Edition*. Hoboken, New Jersey - United States of America: John Wiley & Sons Inc., 2011.

[7] E. Morsch Filho, L. O. Seman, and V. de Paulo Nicolau, "Simulation of a cubesat with internal heat transfer using finite volume method," *Applied Thermal Engineering*, vol. 193, p. 117039, 2021. [Online]. Available: https://www.sciencedirect.com/science/article/pii/S135943112100483X

[8] S. Corpino, M. Caldera, F. Nichele, M. Masoero, and N. Viola, "Thermal design and analysis of a nanosatellite in low earth orbit," *Acta Astronautica*, vol. 115, pp. 247–261, 2015. [Online]. Available: https://www.sciencedirect.com/science/article/pii/S0094576515001940

[9] M. Bulut and N. Sozbir, "Analytical investigation of a nanosatellite panel surface temperatures for different altitudes and panel combinations," *Applied Thermal Engineering*, vol. 75, pp. 1076–1083, 2015. [Online]. Available: https://www.sciencedirect.com/science/article/pii/S1359431114009302

[10] P. Reiss, P. Hager, C. Bewick, and M. MacDonald, "New methodologies for the thermal modeling of cubesats," 06 2012.

[11] J. A. Richmond, "Adaptive thermal modeling architecture for small satellite applications," Ph.D. dissertation, Massachusetts Institute of Technology, 2010.

[12] M. Diaz-Aguado, J. Greenbaum, W. Fowler, and G. Lightsey, "Small satellite thermal design, test, and analysis," *Proceedings of SPIE - The International Society for Optical Engineering*, 05 2006.

[13] R. Lyon, J. Sellers, and C. Underwood, "Small satellite thermal modeling and design at usafa: Falconsat-2 applications," pp. 7–3391, 02 2002.

[14] U. SpaceLab, "GOLDS-UFSC," 2024, https://spacelab.ufsc.br/en/golds-ufsc/.

[15] E. M. Filho, "A coupled irradiance: thermal 3d numerical framework for simulation of cubesats." Ph.D. dissertation, Universidade Federal de Santa Catarina, Florianópolis, Santa Catarina - Brasil, 2021.

[16] D. Bernardi, E. Pawlikowski, and J. Newman, "A general energy balance for battery systems," *Journal of The Electrochemical Society*, vol. 132, no. 1, p. 5, jan 1985. [Online]. Available: https://dx.doi.org/10.1149/1.2113792

[17] Y. Lai, W. Wu, K. Chen, S. Wang, and C. Xin, "A compact and lightweight liquid-cooled thermal management solution for cylindrical lithium-ion power battery pack," *International Journal of Heat and Mass Transfer*, vol. 144, p. 118581, 2019. [Online]. Available: https://www.sciencedirect.com/science/article/pii/S001793101836455X

[18] S. Xin, C. Wang, and H. Xi, "Thermal management scheme and optimization of cylindrical lithium-ion battery pack based on air cooling and liquid cooling," *Applied Thermal Engineering 224 (2023)*, p. 12, 2023.